DESIGN OF DUAL CIRCULARLY POLARIZED AN-TENNA WITH HIGH ISOLATION FOR RFID APPLICA-TION

Xiao-Zheng Lai*, **Ze-Ming Xie, and Xuan-Liang Cen**

School of Computer Science & Engineering, South China University of Technology, Guangzhou 510006, China

Abstract—In this paper, a dual-fed circularly polarized antenna design with high isolation is presented for radio frequency identification (RFID) reader. The proposed antenna is excited by two fed ports connected with a circular split-ring microstrip line underneath the ground plane. A radial aperture in the ground plane provides coupling between the split-ring microstrip and radiating patch. For multiple RFID band requirements, the dimension of the aperture can be modified to obtain high isolation on different RFID Band. Finally, an antenna prototype for China RFID Band (920–925 MHz) is fabricated. The measured results agree well with simulation, and show 10-dB matching bandwidth of 18% (820–1000 MHz), 3-dB axial ratio (AR) bandwidth of 11% (854–960 MHz), and 25-dB isolation bandwidth of 11 MHz (917–928 MHz).

1. INTRODUCTION

The radio frequency identification (RFID) is an automation identification technology that uses radio wave to exchange data between reader and tag attached to an object. Currently, RFID application has seen significant growth in the fields of medicine, security, transportation, logistics, and so on. Antenna design has played a crucial role in the increasing development of RFID technology. Antennas are utilized respectively at the reader and tag, namely reader antenna and tag antenna. The purpose of reader antenna is to process the transmitting (Tx)/receiving (Rx) signal, so the reader can identify the presence of one or several RFID tags. Since tag antennas are normally linearly polarized, circular polarization (CP) radiation of reader antenna is preferred in order to make the identification reliable and more efficient,

regardless of the physical orientation of tag antenna [1]. Circularly-polarized RFID reader antennas with single port have been extensively studied [2–7].

One more important aspect of reader antenna is sufficient isolation between the Tx and Rx signals. RFID system operates in full-duplex mode, and it must transmit continuous wave (CW) in order for the energy and backscattering of the tag. However, the tag's weak backscattered signal is essentially at the same frequency as the reader's strong transmitting CW. Hence, the isolation from Tx to Rx signal can be an important limit of the sensitivity of RIFD reader [8–10]. Although research papers is rare, there have been some partial efforts for this goal. The microwave isolation component, such as circulator, directional coupler or hybrid coupler, is the conventional solution [11–13]. A commercial isolation component generally provides about isolation of 25 dB in the well-matched condition. But, the isolation is critically affected by impedance matching. If the antenna or reader is not well matched with the isolation component, the Tx leakage will be increased. Another guaranteed and low-cost solution is the antenna structure integrated with a branch line coupler as feed network [14, 15]. However, the use of complex branch-line coupler is an inconvenience for mass production and make the overall antenna dimension larger.

Recently, The polarization diversity in one antenna body has been proposed and widely used for location and communication applications, such as satellite navigation, 2G/3G mobile and WLAN system [16–24]. In this paper, a novel dual circularly-polarized antenna design is adopted for RFID reader. The presented antenna structure is based on the aperture coupled patch antenna (ACPA) [25, 26], with separate Tx and Rx port. The radiating patch is fed by a circular split-ring microstrip line, through the aperture ground plane. An antenna prototype is fabricated, and achieves sufficient matching bandwidth and axial ratio bandwidth. Finally, the prototype has better than 25 dB isolation over the China RFID Band (920–925 MHz).

In addition, the RFID technology of ultra-high frequency (UHF) has special frequency allocation for different country: The European Union Nations allows the usage of 865–868 MHz band, while Japan permits 950–956 MHz band. The United States Federal Communications Commission (FCC) designates 902–928 MHz band, and the other country almost approves a part of USA Band for RFID application [27]. Therefore, we adjust the antenna parameters, and successfully obtain good isolation on different RFID band.

The organization of this paper is as follows. The proposed antenna structure with design principle is introduced in Section 2. Section 3

outlines the antenna parametric study. In Section 4, the measured results of prototype are discussed and compared with simulation. The conclusions are given in Section 5.

2. ANTENNA STRUCTURE AND DESIGN

Figure 1 shows the structure of proposed antenna. It consists of a square radiation patch of $L2\,(104\,\text{mm}) \times L2\,(104\,\text{mm})$, which is suspended $H1 = 11\,\text{mm}$ above a ground plane of $L1\,(130\,\text{mm}) \times L1\,(130\,\text{mm})$. The ground plane is printed on the top side of the FR4 substrate ($\varepsilon_r = 4.4$, $\tan\delta = 0.02$, and $H = 1.6\,\text{mm}$), and a circular split-ring microstrip line connects two ports on the bottom side of FR4. The Tx port (#Tx) is on the right side, whereas the Rx port (#Rx) is on the left side. A radial aperture is formed using 12 slots on the ground. These slots are all of equal length $L3$ and width S, and arranged at equal angle intervals. The longitudinal axis of each slot pass through the centre of ground, and a large hole of radius $R2$ is formed in the multiple slot intersection. In Figure 1, the circular spilt-ring microstrip and slots are overlapped to show relative geometrical position between them. It is shown that the centre of hole on the aperture is placed at the centre of circular split-ring, and the length
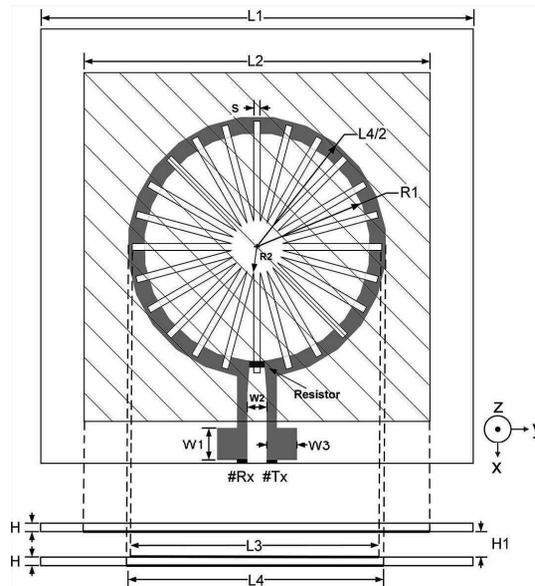

Figure 1. Geometry of the proposed antenna.

$L3$ of slot is approximately equal to the diameter $L4$ of split-ring. The split-ring microstrip pass underneath all the ends of slots, and a $100\,\Omega$ resistor is added on the split of circular ring. The dimension of proposed antenna is as shown in Table 1.

Table 1. Dimension of the proposed antenna (unit: mm).

$L1$	$L2$	$L3$	$L4$	$W1$	$W2$	$W3$	$R1$	$R2$	H	$H1$
130	104	75	78	10	6	9	34	7.6	1.6	10

Simulator Ansoft HFSS ver. 13 is used to analyze the proposed antenna design, at the middle frequency (922 MHz) of China RFID Band (920–925 MHz). The surface current distribution of the split-ring microstrip line and the radial aperture is shown in Figure 2. It can be seen in Figure 2(a) that surface current is flowing along the microstrip line from Tx to Rx port, and gradually attenuated. The current nearby Rx port is greatly weak than that nearby Tx port. As shown in Figure 2(b), The microstrip passes underneath the slots in a serial manner, and generates coupling points at all the end of slots for feeding radiating patch. The slot aperture is equivalent to a defected ground structure (DGS), which has the effect of narrow band rejection filter. These structures enable a sufficient isolation between Tx and Rx port at a certain frequency.
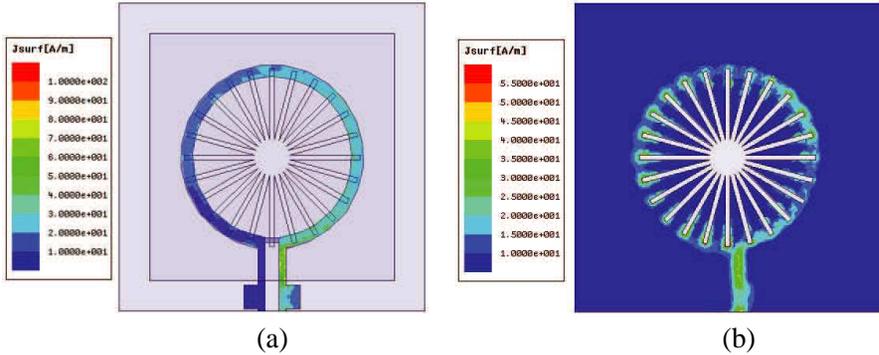

(a)   (b)

Figure 2. Ground plane surface current distribution. (a) Microstrip line on the bottom side, (b) aperture ground on the top side.

The surface current distributions on the radiating patch are shown in Figure 3, at different time frames: $t = 0\,(0°)$, $T/4\,(90°)$, $T/2\,(180°)$, and $3T/4\,(270°)$. It is stated that the Tx port generates Right Hand Circular Polarization (RHCP) by the tip of the current vectors
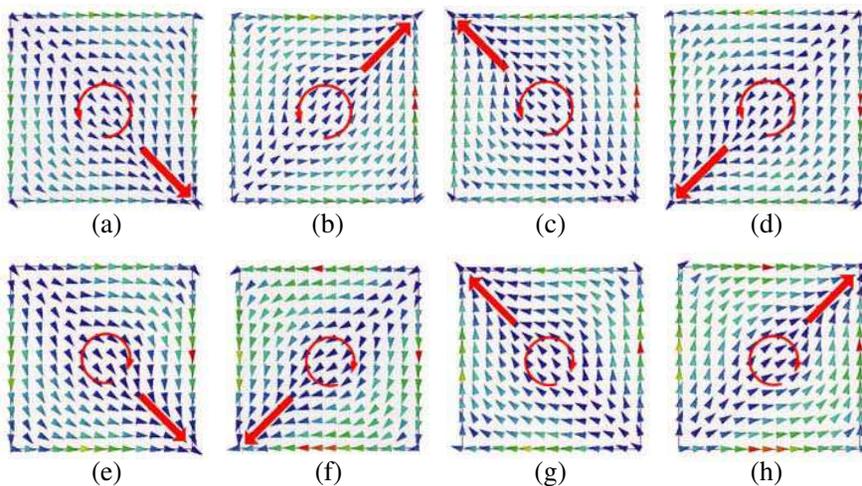
Figure 3. Radiating patch surface current distributions generated by Tx port: (a) 0°, (b) 90°, (c) 180°, (d) 270°, and Rx port: (e) 0°, (f) 90°, (g) 180°, (h) 270°.

(anticlockwise) with time. Since the proposed antenna has a bilaterally symmetrical mirror structure, The Tx and Rx port can interchange to create Left Hand Circular Polarization (LHCP). An opposite rotation (clockwise) for LHCP can similarly be achieved by Rx port. With the proposed antenna, the RFID reader transmits RHCP, while it receives LHCP. Thus, the proposed structure has dual circular polarization in one antenna body, and orthogonal polarization improves isolation between two ports. Since tag antenna generates linear polarization, the RFID communication link is working properly.

3. PARAMETRIC STUDY

This section is intended to give an insight into the antenna behavior of parametric variation. The considered parameters are the presence of RF resistor, the diameter of split-ring microstrip ($L4$), and the width of slot (S) on the ground. In order to keep the relative geometrical position between slots and circular spilt-ring, the length $L3$ of slot is always approximately equal to $L4$, no matter how $L4$ varies. Each of graph shown below exhibits the variation of only one parameter respectively, while others are kept constant.

The first investigated parameter is the resistor added on the split of circular ring. As shown in Figure 4(a), The presence of $100\,\Omega$ resistor
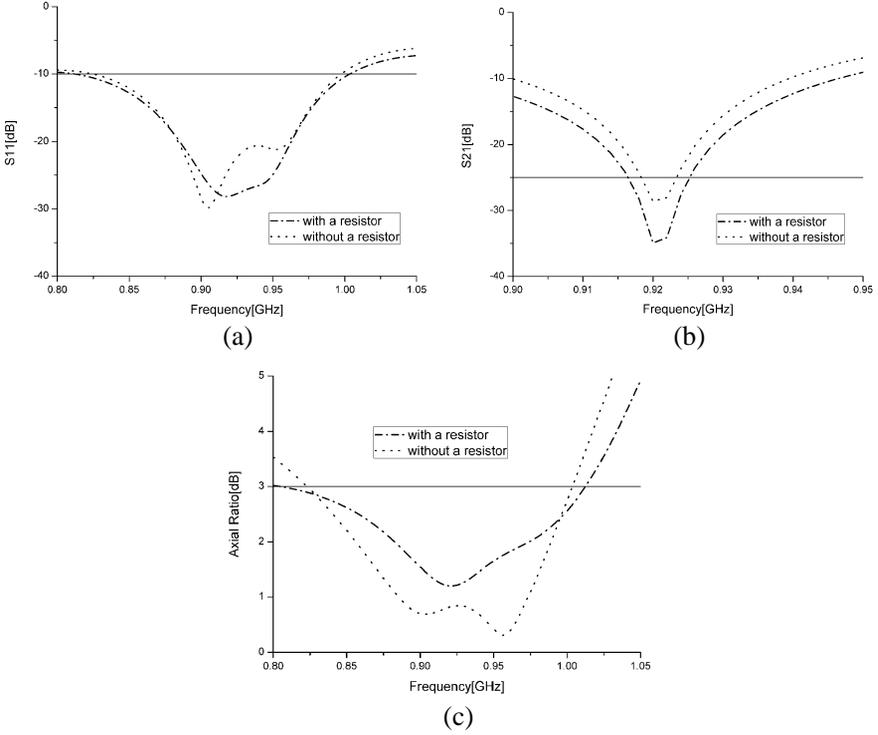
Figure 4. Resistor effect. (a) Reflection coefficient, (b) transmission coefficient, (c) axial ratio.

has a minor effect on the 10-dB matching bandwidth, while 3-dB axial ratio (AR) bandwidth is extended in Figure 4(c). In Figure 4(b), the isolation performance is obviously improved and presents a significant shift down of S_{21} curve. The presence of $100\,\Omega$ resistor enlarge the 25-dB isolation bandwidth from 4 MHz (919–923 MHz) to 8 MHz (917–925 MHz). So, we maintain the presence of resistor in the below simulations and measurements.

A variation by the width S of slot may affect the isolation bandwidth. Figure 5(b) shows that the S_{21} curve shifts slightly in frequency, as the width S is increased from 1 mm to 4 mm. Meanwhile, the 10-dB matching bandwidth still remains 19% (190 MHz), in Figure 5(a). The AR response in Figure 5(c) is mainly affected at the lower end of band, while the change of higher end is small.

The diameter $L4$ of split-ring microstrip has significant effect for isolation performance. It is clearly observed in Figure 6(b) that the S_{21} curve achieves obvious shift in frequency, as the diameter $L4$ is changed

from 76 mm to 80 mm. In any case, the 10-dB matching bandwidth with criteria $S_{11} \leq -10$ dB still remains over 20% (200 MHz) in Figure 6(a). The AR response in Figure 6(c) is mainly affected at
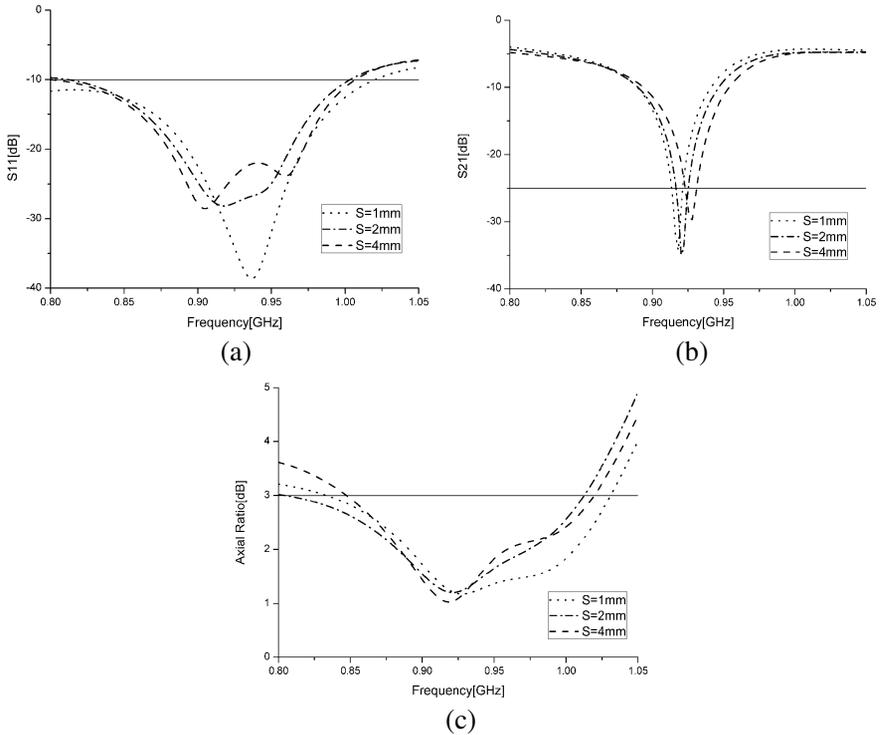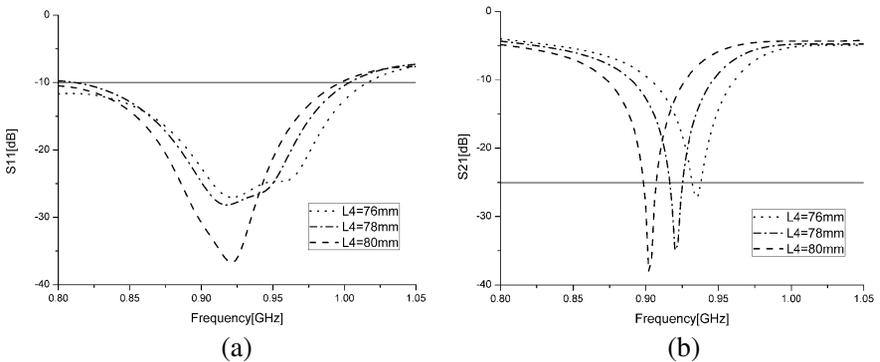

Figure 5. Antenna behavior with different slot width S. (a) Reflection coefficient, (b) transmission coefficient, (c) axial ratio.
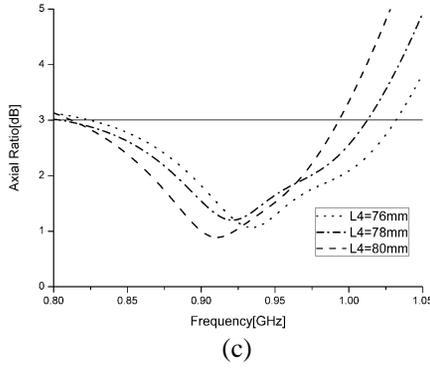
(c)

Figure 6. Antenna behavior with different split-ring diameter $L4$. (a) Reflection coefficient, (b) transmission coefficient, (c) axial ratio.
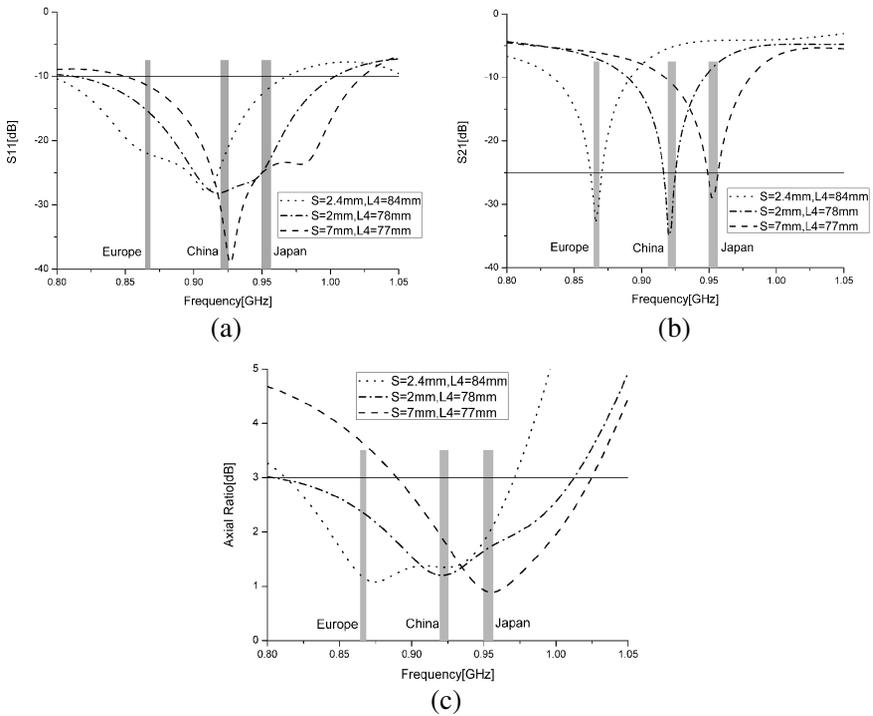

(a)

(b)

(c)

Figure 7. Parametric study results for different RFID band. (a) Reflection coefficient, (b) transmission coefficient, (c) axial ratio.

the higher end of band, while the change of lower end is small.

Through numerous simulations, we can find that the width S of slot and diameter $L4$ of split-ring are paramount factors and needs serious consideration for isolation bandwidth of different RFID band. Figure 7 show parametric study results: In order to cover Europe Band (865–868 MHz), $S = 2.4$ mm and $L4 = 84$ mm are applied. Furthermore, $S = 7$ mm and $L4 = 77$ mm are used for Japan Band (952–954 MHz). Finally, the designed parameters for China Band (920–925 MHz) are $S = 2$ mm and $L4 = 78$ mm. For clearly visualization, the shadow region of the below graphs represents the interest RFID band.

Considering the simulation for China Band (920–925 MHz), a 25-dB isolation bandwidth of 8 MHz (917–925 MHz) is obtained. Meanwhile, the 10-dB matching bandwidth is 190 MHz (812–1002 MHz), and 3-dB AR bandwidth is 206 MHz (806–1012 MHz). The matching and AR bandwidth are both sufficient to cover Europe, China and Japan RFID band, simultaneously.

4. MEASURED RESULTS

A proposed antenna prototype for China Band (920–925 MHz) is fabricated. The top, bottom and side view of prototype are displayed on Figures 8(a), (b) and (c). For convenience in fabrication process, the FR-4 substrate with microstrip line and ground plane is sitting on a 11 mm thick layer by foam support above the patch substrate. Figure 9 shows the antenna under test (AUT) placed inside the anechoic chamber for radiation pattern and axis ratio pattern measurements. The test setup uses a linear spinning antenna as probe antenna in the measurements.
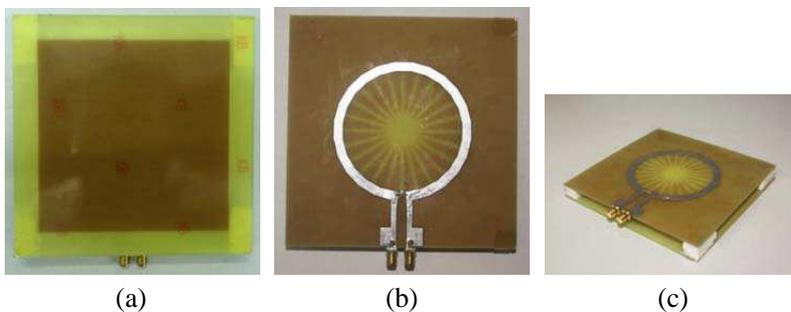

(a)   (b)   (c)

Figure 8. Antenna prototype. (a) Top view, (b) bottom view, (c) side view.

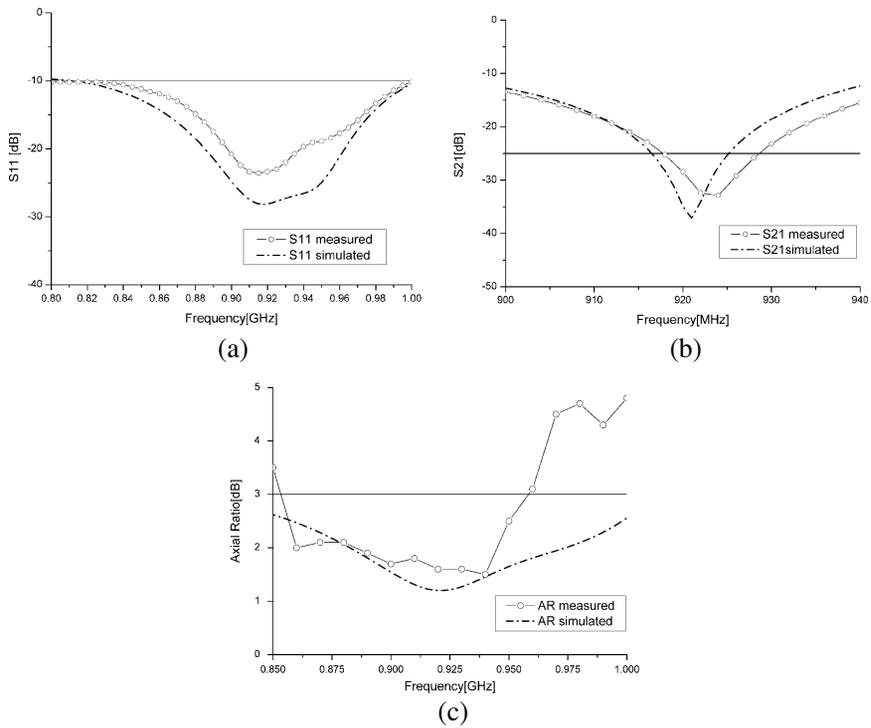**Figure 9.** Antenna under test (AUT) in chamber.

(a)

(b)

(c)

Figure 10. Measured and simulated antenna behaviors. (a) Reflection coefficient, (b) transmission coefficient, (c) axial ratio.

The measured reflection and transmission coefficients with simulation are shown in Figures 10(a) and (b), respectively. The measured reflection coefficient magnitude ($S_{11} \leq -10\,\text{dB}$) presents a bandwidth of $180\,\text{MHz}$ (820–$1000\,\text{MHz}$), which yields a percentage

bandwidth of 18%. The measured transmission coefficient magnitude ($S_{21} \leq -25$ dB) presents a bandwidth of 11 MHz (917–928 MHz), which covers the China (920–925 MHz), Korea (917–924 MHz) and Australia (918–926 MHz) RFID Band. Figure 10(c) shows the measured AR response compared to the simulated results. The measured AR bandwidth (AR $\leq$ 3 dB) presents a bandwidth of 106 MHz (854–960 MHz).

Figure 11 shows the axial ratio pattern at 922 MHz. The axial ratio was smaller than 3.0 dB over 85° in the upper hemisphere on the *xoz*-plane. A similar axial ratio performance was observed over 100° on the *yoz*-plane.
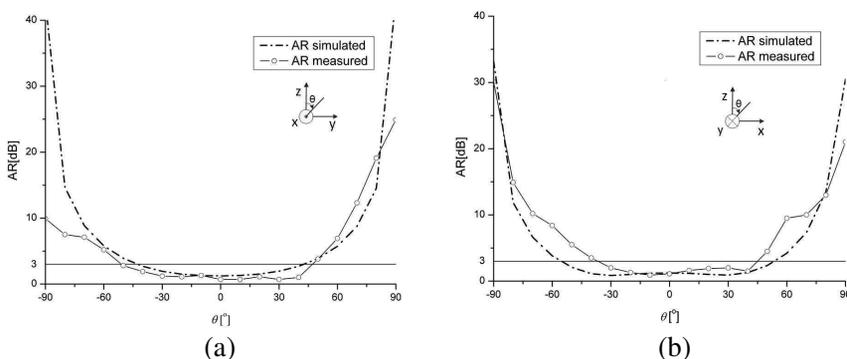

Figure 11. Simulated and measured axis ratio patterns at 922 MHz.

The normalized simulated and measured radiation patterns at 922 MHz are plotted in the two orthogonal planes (*xoz*-plane and *yoz*-plane), as shown in Figure 12. The measured maximum RHCP gain is obtained at the positive *Z*-axis, while measured maximum LHCP gain at the negative *Z*-axis. The measured RHCP radiation patterns have a fairly wide 3 dB-beamwidth of 80°, which suggest wide angular coverage as expected for RFID reader. The measured RHCP gain has the maximum of 4.3 dBic in *xoz*-plane, and 4.9 dBic in *yoz*-plane, respectively. The measured LHCP gain has the maximum of −2.0 dBic in *xoz*-plane, and −2.2 dBic in *yoz*-plane, respectively.

Finally, to examine the antenna performance, experiments on tag reading at 922 MHz have been performed. Since the commercial RFID system often integrates circulator and has only one antenna port, we use Tektronix Real-time Spectrum Analyzer (RSA) 3303A [28] as reference reader to compare the performance of proposed antenna and standard antenna with a common circulator. The circulator has at least 23 dB isolation in the frequency range 920–925 MHz. The standard
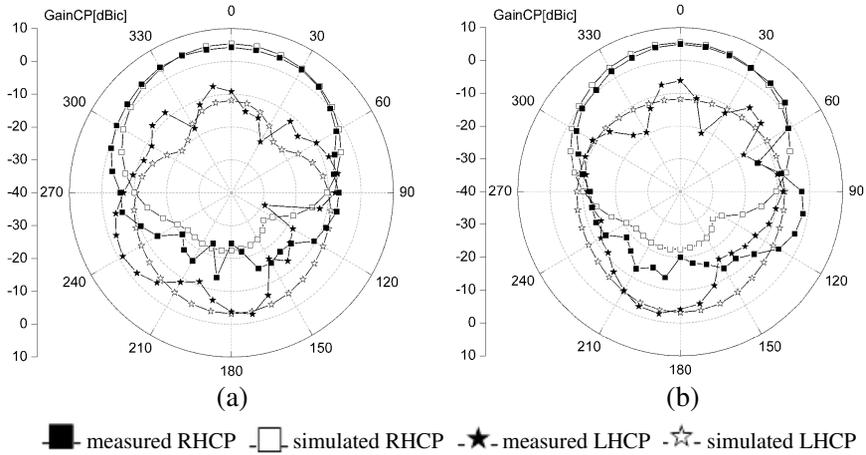
Figure 12. Simulated and measured radiation patterns at 922 MHz. (a) *xoz*-plane, (b) *yoz*-plane.

antenna has a RHCP gain of 5.0 dBic, and the proposed antenna has a RHCP gain of 4.9 dBic.

With 23-dB circulator, the standard antenna can detect a reference UHF RFID tag (Impinj tag [29]) up to 7.8 m, under the transmission power level of 27 dBm (0.5 W). Measurements also show that the proposed antenna has a maximum readable range of 8.1 m, with the same RFID tag and under the same transmission power level. So we can use the proposed antenna instead of a standard antenna with a common circulator in a complete RFID system.

5. CONCLUSIONS

In this work, a novel RFID reader antenna with dual polarization and high isolation is proposed. The antenna consists of a separate radiating patch and an aperture-coupled ground plane. The radiating patch is fed by a circular split-ring microstrip line through the aperture ground. A compact antenna size, dual-port-isolation better than 25 dB and good circular polarization are achieved by proposed structure without using microstrip branch line coupler or other complex feed networks. Detailed parametric study was discussed, such as the presence of resistor, the diameter of split-ring microstrip, and the width of slot on the aperture. These antenna parameters can be varied to realize optimized isolation bandwidth for different RFID band.

An antenna prototype for China Band (920–925 MHz) was

fabricated and measured, which showed good agreement with simulation. The prototype presents 10-dB matching bandwidth of 18% (820–1000 MHz), 3-dB AR bandwidth of 11% (854–960 MHz), and 25-dB isolation bandwidth of 11 MHz (917–928 MHz). The maximum measured RHCP gains are 4.3 dBic in *xoz*-plane, and 4.9 dBic in *yoz*-plane. Such proposed antenna can serve as a good candidate for RFID reader installations.

ACKNOWLEDGMENT

REFERENCES

1. Glover, B. and H. Bhatt, *RFID Essentials*, O'Reilly, Sebastopol, CA, 2006.

2. Chen, X., G. Fu, S. X. Gong, Y. L. Yan, and W. Zhao, "Circularly polarized stacked annular-ring microstrip antenna with integrated feeding network for UHF RFID readers," *IEEE Antennas and Wireless Propagation Letters*, Vol. 9, 542–545, Jun. 2010.

3. Deng, J.-Y., L.-X. Guo, T.-Q. Fan, Z.-S. Wu, Y.-J. Hu, and J.-H. Yang, "Wideband circularly polarized suspended patch antenna with indented edge and gap-coupled feed," *Progress In Electromagnetics Research*, Vol. 135, 151–159, 2013.

4. Wang, P., G. Wen, J. Li, Y. Huang, L. Yang, and Q. Zhang, "Wideband circularly polarized UHF RFID reader antenna with high gain and wide axial ratio beamwidths," *Progress In Electromagnetics Research*, Vol. 129, 365–358, 2012.

5. Tiang, J.-J., M. T. Islam, N. Misran, and J. S. Mandeep, "Circular microstrip slot antenna for dual-frequency RFID application," *Progress In Electromagnetics Research*, Vol. 120, 499–512, 2011.

6. Chang, T. N. and J. M. Lin, "Circularly polarized ring-patch antenna," *IEEE Antennas and Wireless Propagation Letters*, Vol. 11, 26–29, 2012.

7. Ooi, P. C. and K. T. Selvan, "A dual-band circular slot antenna with an offset microstrip-FED line for PCS, UMTS, IMT-2000, ISM, bluetooth, RFID and WLAN applications," *Progress In Electromagnetics Research Letters*, Vol. 16, 1–10, 2010.

8. Fan, Z., S. Qiao, J. T. Huang-Fu, and L.-X. Ran, "Signal descriptions and formulations for long range UHF RFID readers," *Progress In Electromagnetics Research*, Vol. 71, 109–127, 2007.

9.   Kim, D.-Y., H.-G. Yoon, B.-J. Jang, and J.-G. Yook, "Interference analysis of UHF RFID systems," *Progress In Electromagnetics Research B*, Vol. 4, 115–126, 2008.

10. Lazaro, A., D. Girbau, and R. Villarino, "Effects of interferences in UHF RFID systems," *Progress In Electromagnetics Research*, Vol. 98, 425–443, 2009.

11. Lim, W. G., S. Y. Park, and W. I. Son, "RFID reader front-end having robust Tx leakage canceller for load variation," *IEEE Transactions on Microwave Theory and Techniques*, Vol. 57, No. 5, 1348–1355, 2009.

12. Bae, J.-H., W.-K. Choi, J.-S. Kim, G.-Y. Choi, and J.-S. Chae, "Study on the demodulation structure of reader receiver in a passive RFID environment," *Progress In Electromagnetics Research*, Vol. 91, 243–258, 2009.

13. Kim, W. K., W. Na, and J. W. Yu, "A high isolated coupled-line passive circulator for UHF RFID reader," *Microwave and Optical Technology Letters*, Vol. 50, No. 10, 5297–2600, 2008.

14. Mireles, E. and S. K. Sharma, "A novel wideband circularly polarized antenna for worldwide UHF band RFID reader applications," *Progress In Electromagnetics Research B*, Vol. 42, 23–44, 2012.

15. Jung, Y. K. and B. Lee, "Dual-band circularly polarized microstrip RFID reader antenna using metamaterial branch-line coupler," *IEEE Transactions on Antennas and Propagation*, Vol. 60, No. 2, 786–791, 2012.

16. Secmen, M. and A. Hizal, "A dual-polarized wide-band patch antenna for indoor mobile communication applications," *Progress Progress In Electromagnetics Research*, Vol. 100, 189–200, 2010.

17. Yao, Y., X. Wang, X. D. Chen, J. S. Yu, and S. H. Liu, "Novel diversity/MIMO PIFA antenna with broadband circular polarization for multimode satellite navigation," *IEEE Antennas and Wireless Propagation Letters*, Vol. 11, 65–68, 2011.

18. Vongsack, S., C. Phongcharoenpanich, S. Kosulvit, K. Hamamoto, and T. Wakabayashi, "Unidirectional antenna using two-probe excited circular ring above square reflector for polarization diversity with high isolation," *Progress In Electromagnetics Research*, Vol. 133, 159–176, 2013.

19. Xie, J.-J., Y.-Z. Yin, J. Ren, and T. Wang, "A wideband dual-polarized patch antenna with electric probe and magnetic loop feeds," *Progress In Electromagnetics Research*, Vol. 132, 499–515, 2012.

20. Segovia-Vargas, D., F. J. Herraiz-Martinez, E. Ugarte-Munoz, L. E. Garcia-Munoz, and V. Gonzalez-Posadas, "Quad-frequency linearly-polarized and dual-frequency circularly-polarized microstrip patch antennas with CRLH loading," *Progress In Electromagnetics Research*, Vol. 133, 91–115, 2013.

21. Liu, C., J.-L. Guo, Y.-H. Huang, and L.-Y. Zhou, "A novel dual-polarized antenna with high isolation and low cross polarization for wireless communication," *Progress In Electromagnetics Research Letters*, Vol. 32, 129–136, 2012.

22. Krairiksh, M., P. Keowsawat, C. Phongcharoenpanich, and S. Kosulvit, "Two-probe excited circular ring antenna for MIMO application," *Progress In Electromagnetics Research*, Vol. 97, 417–431, 2009.

23. Wu, G.-L., W. Mu, G. Zhao, and Y.-C. Jiao, "A novel design of dual circularly polarized antenna FED by L-strip," *Progress In Electromagnetics Research*, Vol. 79, 39–46, 2008.

24. Chou, H.-T., H.-C. Cheng, H.-T. Hsu, and L.-R. Kuo, "Investigations of isolation improvement techniques for multiple input multiple output (MIMO) WLAN portable terminal applications," *Progress In Electromagnetics Research*, Vol. 85, 349–366, 2008.

25. Zhang, M. T., Y. B. Chen, Y. C. Jiao, and F. S. Zhang, "Dual circularly polarized antenna of compact structure for RFID application," *Journal of Electromagnetic Waves and Applications*, Vol. 20, No. 14, 1895–1902, 2006.

26. Chang, T. N. and J. M. Lin, "A novel circularly polarized patch antenna with a serial multislot type of loading," *IEEE Transactions on Antennas and Propagation*, Vol. 55, No. 11, 3345–3348, 2007.

27. Paret, D., *RFID at Ultra and Super High Frequencies Theory and Application*, 2nd Edition, Wiley, United Kingdom, 2009.

28. Online available: http://www.tek.com/sites/tek.com/files/media /media/resources/37W_18864_2.pdf.

29. Online available: http://www.rfidinfo.jp/whitepaper/379.pdf.